AIAA 80-0310R

Investigation of Delta Wing Leading-Edge Devices

Dhanvada M. Rao*
Vigyan Research Associates, Inc. Hampton, Va.
and
Thomas D. Johnson Jr.†
Kentron International, Inc., Hampton Technical Center, Hampton, Va.

Leading-edge flow manipulators for alleviating the subsonic lift-dependent drag of highly-swept wings were investigated experimentally. The potential of several devices—fences, chordwise slots, pylon vortex generators, and a vortex plate concept—was evaluated in wind tunnel tests on a 60 deg cropped delta wing research model. Simultaneous balance and pressure measurements at increasing angles of attack provided an insight into the spanwise leading-edge flow development and its modification by the devices. The results demonstrated significant drag reductions through partial recovery of leading-edge suction at elevated angles of attack. In most cases, improvement in longitudinal stability also was obtained.

Nomenclature

C_A = axial or chord force coefficient
$C_{A,0}$ = axial or chord force coefficient at zero lift
C_D = drag coefficient
$C_{D,b}$ = drag coefficient of basic wing (devices off)
ΔC_D = drag increment with devices $= C_D - C_{D,b}$
C_m = pitching moment coefficient (about moment center shown in Fig. 2)
C_N = normal force coefficient
C_P = pressure coefficient
C_l = local leading-edge thrust coefficient at a spanwise station (obtained from pressure integration)
C_T = total leading-edge thrust coefficient (summation of C_l from all spanwise pressure stations, accounting for total wing span)
$C_{T,\,VL}$ = total leading-edge thrust coefficient by vortex lattice method
α = angle of attack
η = spanwise distance from wing centerline as a fraction of semispan

Introduction

HISTORICALLY the delta wing has been developed for its favorable supersonic drag characteristics. The relatively poor low-speed aerodynamic efficiency of such wings could be tolerated as long as it was encountered only during takeoff and landing when excess power usually is available. Currently, however, a high order of subsonic maneuverability is in demand for combat aircraft designed for supersonic cruise. A highly swept delta is a logical choice for such advanced aircraft as it combines the advantages of low wave drag at cruise with high g subsonic maneuver capability due to vortex lift. Vortex lift is costly in terms of drag however, and its exploitation for maneuver may therefore be constrained by engine thrust (or fuel consumption if afterburner is employed). The alternative is to attempt an extension of the angle-of-attack range of potential flow (i.e., with full leading-edge suction to counteract the pressure drag) by appropriate control of the leading-edge flow.

A prerequisite for attached flow is leading-edge bluntness. Although they may appear out of place on a supersonic wing, blunt leading edges swept behind the Mach cone potentially can improve supersonic cruise efficiency through recovery of leading-edge suction.[1] Thus it seems worthwhile to explore the prospects of retaining attached leading-edge flow to elevated angles of attack for enhanced subsonic maneuver capability of highly swept wings.

Published literature offers little evidence of attempts at, or success in, controlling leading-edge separation with sweep angles exceeding about 40 deg. Up to this degree of sweep, leading-edge slots and flaps have proven effective. At sweep angles of 60 deg and more, typical of supersonic-cruise designs, the highly three-dimensional flow around the leading-edge with pronounced spanwise velocity component renders the basis of such devices (which fundamentally represent a two-dimensional approach) questionable. From a practical viewpoint, the high g and dynamic pressure environment of combat maneuver will subject the flap and slot type structures and their supports to distortion effects and complicate their actuation requirements.

Experience with fixed devices such as leading-edge fences to control swept-wing stall behavior[2] has shown that they profoundly influence the spanwise development of leading-edge flow separation. Although frequently employed as "fixes" to cure longitudinal stability problems, fences have not been investigated as possible means of high-alpha drag reduction of highly swept wings. This paper explores the potential of fences and three other novel leading-edge flow manipulators in the role of drag-reduction devices. These devices were evaluated on a 60 deg cropped delta wing model in subsonic wind-tunnel tests. Analyses of pressure and force measurements are presented to illustrate the unique aerodynamic features of the various devices and their impact on the high-alpha drag as well as longitudinal stability characteristics.

Leading-Edge Devices

The particular devices of the present investigation are sketched in Fig. 1 and briefly discussed in the following.

Fences

The underlying aerodynamic mechanism of chordwise fences placed on a swept leading edge has been discussed in Ref. 3. In essence, the isobars normally swept parallel to the leading edge are forced to unsweep locally due to a partial reflection-plane effect of the fence. The effects are opposite

Received Jan. 9, 1980; presented as Paper 80-0310 at the AIAA 18th Aerospace Sciences Meeting, Pasadena, Calif., Jan. 14-16, 1980; revision received July 7, 1980.

*President. Member AIAA.
†Aerodynamics Engineer.

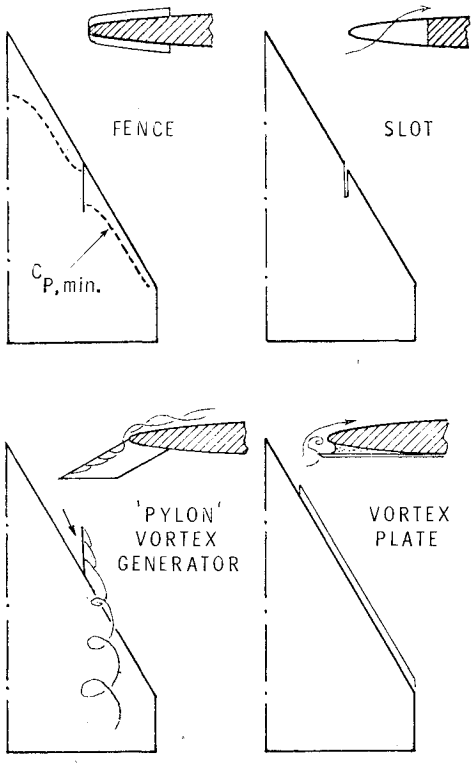

Fig. 1 Leading-edge device concepts.

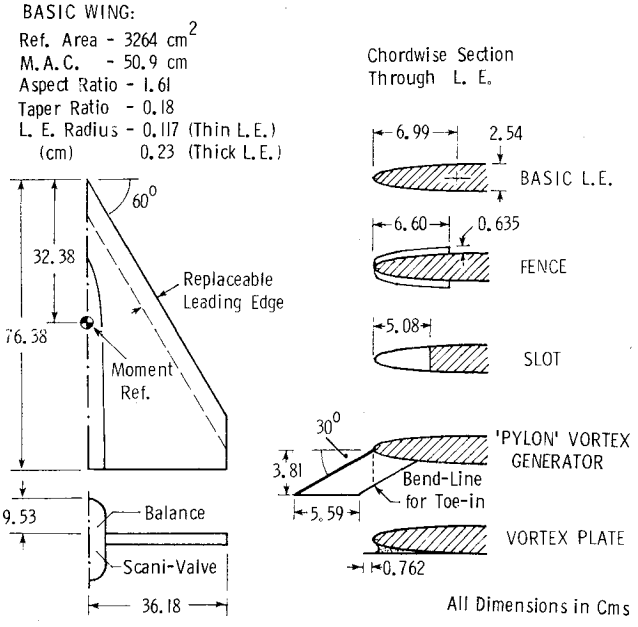

Fig. 2 Delta wing model and devices: geometry and dimensions.

on either side of the fence: the leading-edge suction peaks and pressure-recovery gradients are accentuated inboard but relieved outboard. On the outboard regions of the wing prone to early separation, this has the effect of a positive leading-edge camber and accordingly the stall onset is delayed to a higher angle of attack. The negative camber effect induced inboard is less of a concern due to the smaller leading-edge upwash prevailing there. The fence also partially blocks the spanwise boundary-layer flow and thus further alleviates the tendency for early tip stall on the plain wing. With a number of fences suitably distributed spanwise, attached flow may be maintained to a higher angle of attack over a substantial fraction of the span. Obviously, the size, number and distribution of the fences will have to be optimized in order to keep the cruise drag penalty within acceptable limits.

Chordwise Slots

It was hypothesized that the three-dimensional effects on a swept leading edge might be suppressed by compartmenting it into a number of two-dimensional segments and thus the stall angle of the wing improved. The high-velocity fluid sheets issuing out of chordwise slots cut into the leading edge (due to natural flow venting at high angles of attack) were expected to accomplish the desired effect by acting somewhat like aerodynamic fences. The slots already provided in the wing model for the purpose of holding the fences and other devices (and normally sealed when not in use) were expediently utilized to explore this concept.

Pylon Vortex Generators

The traditional surface-mounted vortex generators, long used in aerodynamics practice to cure unexpected flow separation problems, essentially are boundary-layer energizers. The present device, on the other hand, utilizes the induced velocity field of a free vortex originating upstream of the leading edge to modify the spanwise upwash distribution such as to retard the onset of leading-edge separation. The top edge of a swept-forward pylon-shaped blade functions as a separation edge for the lateral velocity component in the flow approaching the wing leading edge. The rotational sense of the resulting vortex is such as to relieve the leading-edge load over the outboard portion of the wing thereby delaying the stall onset. Except at the lowest angles of attack, the vortex will be lifted over the leading edge and therefore a degree of boundary-layer energization on the upper surface may be expected to further assist in delaying separation.

Vortex Plate

The common basis of the devices just described is to maintain attached leading-edge flow over a large fraction of the wing span and thereby retain a large measure of the potential-flow suction to higher angles of attack. As a radical departure from that approach, the vortex plate operates by forcing separation in order to generate a spanwise vortex just in front of the leading edge, and utilize its suction effect to obtain a thrust force. The separation edge in this case is provided by a narrow sharp-edge plate projecting forward from under the leading edge and swept parallel to it. The sweep angle serves to stabilize the vortex and promotes its persistence in the spanwise direction. Ideally, the vortex size and position should be such that the associated flow attachment occurs just aft of the leading-edge curvature in order to avoid local suction peaks and the possibility of separation on the wing over a desired angle-of-attack range. Although modeled as a fixed plate in this investigation, the device easily may be designed to be retractable in order to avoid cruise drag penalty.

Experimental Details

The delta wing model of wooden construction (Fig. 2) was basically a flat plate with two interchangeable pairs of leading edges, 1.27 and 2.54 cm in thickness referred to as "thin" and "thick," respectively. The two leading-edge designs were of uniform semielliptical cross section with major-to-minor axis ratio 5.5, differing only in scale. The "thin" leading edge was solid whereas the "thick" leading edge contained chordwise rows of static pressure orifices (at semispan stations $\eta = 0.2$, 0.33, 0.45, 0.57, 0.7 and 0.82), distributed around the nose from top to bottom in order to facilitate calculation of the local thrust force by pressure integration. Chordwise slots were cut into the leading edges at stations $\eta = 0.25$, 0.375, 0.5, 0.625, 0.75 and 0.875 to accommodate the devices. The slots not in use were sealed flush with the wing surface. A sting-supported, six-component strain-gage balance was mounted on the top of the wing and two pressure-scanning valves located at the bottom. Symmetrical shields were provided to cover the instrumentation.

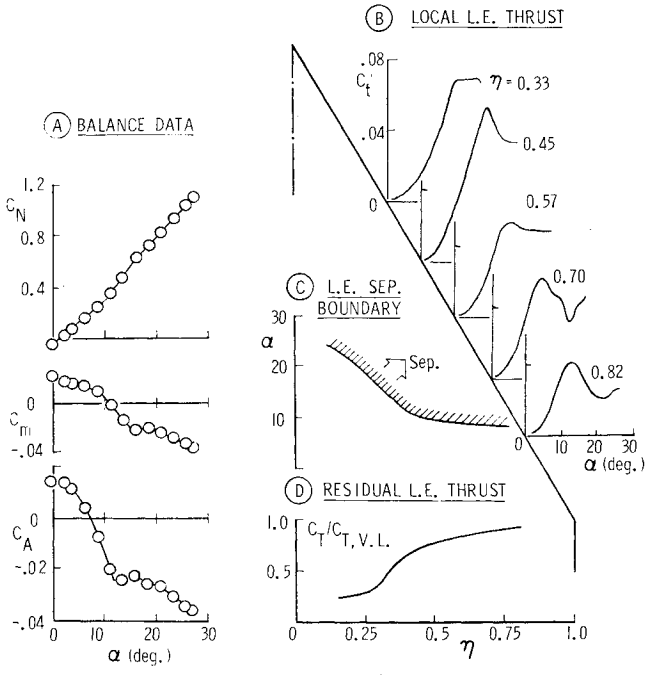

Fig. 3 Basic wing aerodynamic characteristics.

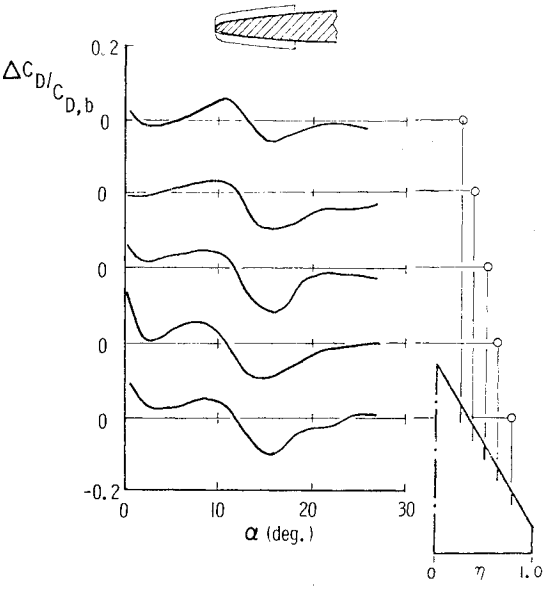

Fig. 4 Drag reduction with a single fence at various spanwise positions.

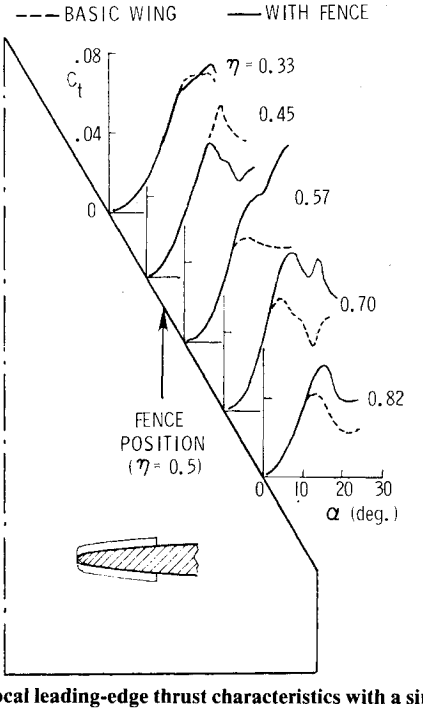

Fig. 5 Local leading-edge thrust characteristics with a single fence.

The geometry and dimensions of the leading-edge devices shown in Fig. 2 represent the best from each category, selected on the basis of overall drag-reduction performance through preliminary screening tests. The full range of devices investigated together with tabulated test data will be found in Ref. 4. The fences and pylon vortex generators were cut from 1 mm thick aluminum sheet while the vortex plate was made of 2 mm aluminum plate. The devices were generally small in size relative to the wing; for example, each pylon vortex generator was about 0.5% of the wing reference area, and the chordwise projection of the vortex plate ahead of the leading edges was 3% of mean aerodynamic chord.

The tests were conducted in NASA Langley 7×10-ft wind tunnel at a nominal Mach number of 0.16 and Reynolds number of 2.0×10^6 based on mean chord. The balance axial (chord) force measurement were corrected to zero base drag on the housing cross-sectional area. Corrections for sting and balance deflections were applied to angle of attack.

Discussion of Results

The basic wing characteristics first will be presented to establish a reference. The drag-reduction performance of the different devices relative to the basic wing derived from balance measurements will be discussed in turn. Typical leading-edge thrust characteristics determined from pressure measurements will be presented to illustrate some of the unique features of each concept. Finally, the effect of leading-edge devices on longitudinal stability will be noted.

Basic Wing

The normal force, pitching moment, and chord force characteristics of the basic delta wing (thick leading edges) are presented in Fig. 3a. From the breaks in these data, three different stages in the growth of separation with angle of attack may be identified. Separation first occurs off the lower edge of the streamwise tips, the resulting vortex moving over to the upper surface at about $\alpha=8$ deg to generate vortex lift in conjunction with a nose-down moment as evident in the C_N and C_M data, respectively. There is no break at this point in C_A characteristics since streamwise tip separation does not affect the chord force. By about 10 deg angle of attack, leading-edge separation has grown sufficiently to produce the large reduction in leading-edge thrust indicated by C_A data.

The continuing spread of leading-edge separation toward the wing apex and increase of vortex lift at higher angles of attack moves the lift center ahead of c.g. to cause a "pitchup" and reduction in stability starting at about $\alpha=16$ deg. (A contributory factor may be vortex breakdown, the effect of which is first felt at about $\alpha=16$ deg on a 60 deg delta with sharp leading edges; the influence of bluntness on delta wing vortex breakdown however is not known.)

Further insight into the development of leading-edge separation and associated thrust loss is provided by the local thrust characteristics (C_t) obtained from integrated pressures around the leading edge at several spanwise stations (see Fig. 3b). Initially, C_t increases in proportion to $\sin^2\alpha$ (as in potential flow) up to an angle of attack corresponding to onset of separation. The departure angle of attack as a function of semispan position yields a separation boundary plotted in Fig. 3c. This boundary indicates that leading-edge

separation starting around $\alpha = 9$ deg at the tip rapidly spreads inboard to about 0.45 semispan position (in less than 2 deg increment from the onset angle of attack) but slows down thereafter, crossing $\eta = 0.25$ station at about 20 deg angle of attack.

The residual leading-edge thrust on the whole wing after onset of separation (obtained by spanwise summation of the local thrust values at given angles of attack beyond departure), normalized by the calculated total thrust by vortex lattice method[5] is plotted directly below the separation boundary (Fig. 3d). A noteworthy feature is the relatively slow rate of thrust loss until separation has moved inboard of approximately the mid-semispan position. It may be concluded that any device arrangement that is able to contain leading-edge separation to the outboard half of the wing panel should produce significant high-alpha drag reduction on this wing.

The drag reduction ΔC_D due to a leading-edge device will be a function of angle of attack. Starting with the angle of attack for onset of separation on the basic wing, the drag reduction will reach a peak just before the effectiveness of the separation-control device begins to break down, eventually dropping off to zero. At low angles of attack where the basic wing still has attached leading-edge flow, a drag penalty due to the device will appear. The merit of a particular fixed device must be judged on an overall basis considering its performance through the angle-of-attack range of interest.

Fences

The drag-reduction sensitivity to spanwise location of a single fence is illustrated by data obtained with progressively increasing spanwise distance, Fig. 4. The best performance overall is obtained with the fence at 50% semispan. The low-alpha drag penalty worsens with increasingly outboard location of the fence.

The local leading-edge thrust characteristics at different spanwise stations showing the effect of a single fence placed at 50% semispan are presented in Fig. 5. Of particular interest are the stations closest to the fence where the underlying flow mechanism clearly is evident in the data, viz., earlier stall inboard but delayed outboard. It is noteworthy that while the adverse effect is confined to the closest inboard station, the benefit due to the fence extends to all the outboard stations. This may be ascribed to a piling up of low energy boundary-layer fluid at the inboard side of the fence whereas outboard a thinner boundary layer results.

The leading-edge separation boundary derived from local thrust characteristics with a single fence at 50% semispan is compared with the basic wing, Fig. 6a. The fence appears to split the separation boundary, the inner half being pushed down while the outer half is raised to higher angles of attack, in accordance with the aerodynamic mechanism already described. The effect is even more pronounced when three fences are employed at uniform spacing across the semispan, as indicated in Fig. 6b. With three fences, over 75% of the leading-edge length has attached flow at $\alpha = 15$ deg for example, as against 50% with a single fence and 30% on the basic wing. The implications of this leading-edge flow improvement in terms of drag reduction are shown in Fig. 6c; three fences produce almost twice the drag reduction of a single fence at $\alpha = 15$ deg and also their effectiveness is better maintained at higher angles of attack. Further improvement in the fence effectiveness may be possible through measures to eliminate the adverse flow inboard, e.g., by local leading-edge camber or an adjacent chordwise slot to "blow off" the viscous accumulation.

Slots

The drag reduction achieved by opening up increasing number of chordwise slots is shown in Fig. 7. These data were obtained on the thin leading-edge model where flow separation and drag rise occurred earlier, which explains the

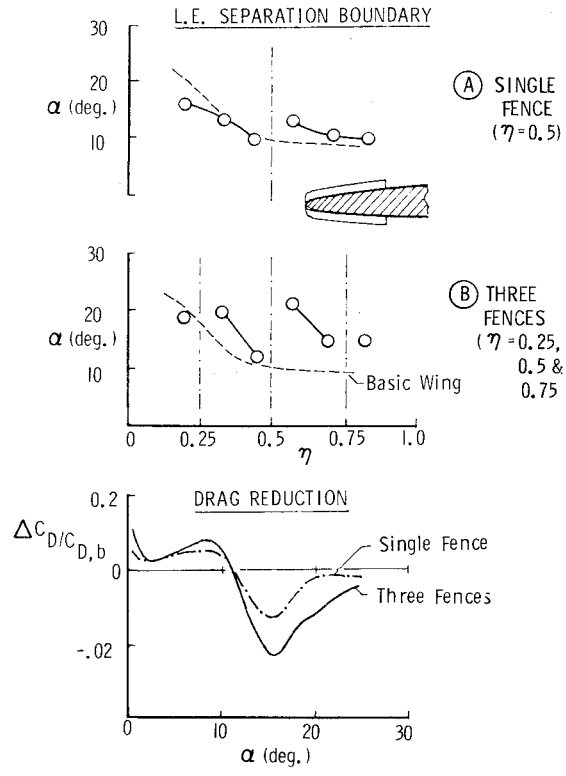

Fig. 6 Leading-edge separation boundaries and drag reduction with single and three fence arrangements.

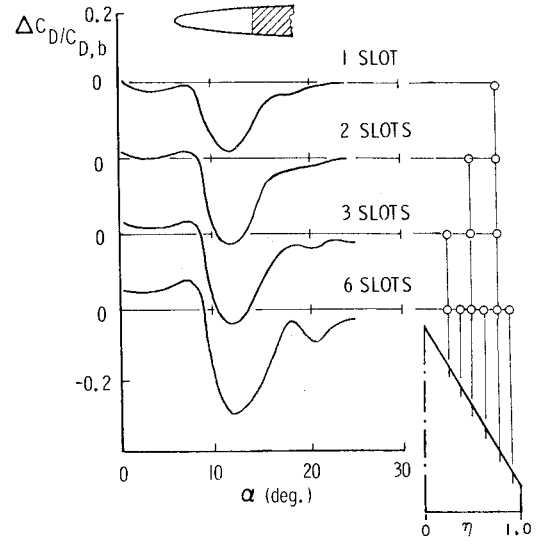

Fig. 7 Drag reduction with increasing number of chordwise slots.

earlier peaking of the drag-reduction performance, viz., at $\alpha = 12$ deg in this case (vs 15 deg on the thick leading-edge model). As the number of slots increases so does the peak drag reduction, but with increasing low-alpha drag penalty particularly when more than three slots are used. Presumably, a major part of the low-alpha drag arises from the positive pressures on the vertical face at the end of the slots, which could be alleviated by internal streamlining.

The local leading-edge thrust characteristics with five slots on the thick leading-edge wing are presented in Fig. 8. Considerably improved thrust peaks at all stations followed by an abrupt collapse almost simultaneously across the semispan, indicated that the slots indeed were effective in compartmenting the leading edge into segments, each having a two-dimensional airfoil type leading-edge stall. It is likely that a more realistic wing with spanwise variation of leading-

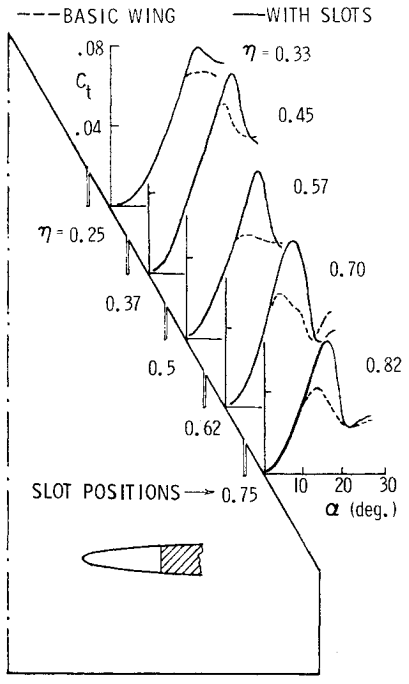

Fig. 8 Local leading-edge thrust characteristics with slots.

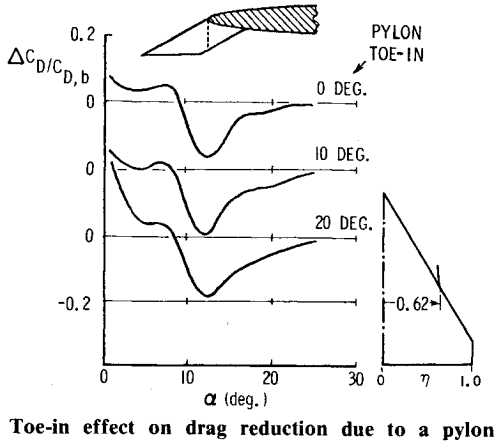

Fig. 9 Toe-in effect on drag reduction due to a pylon vortex generator.

edge radius (unlike the present uniform geometry) will produce a more progressive stall of the segments.

Pylon Vortex Generator

Since it utilizes the sidewash component of the incident flow for vortex production, the pylon toe angle should be important to its performance. The "flat" pylons initially tested were observed to bend outward into a toe-out configuration under aerodynamic load. While this did not interfere with the high-alpha drag-reduction capability of the device, as shown by the top curve in Fig. 9, an excessive drag penalty was incurred at low angles of attack. A 10 deg toe-in bend applied to the pylons largely eliminated the aeroelastic deflection. As a result, the low-alpha drag was reduced significantly and the drag-reduction performance at the higher angles of attack was improved as well. With the toe in increased further to 20 deg however, the low-alpha penalty reappeared. All subsequent tests were carried out with the pylon vortex generators bent to a 10 deg toe-in angle.

The effect of spanwise position on the drag reduction due to a single pylon vortex generator is presented in Fig. 10. From these and other data (not shown) the best drag-reduction performance with a single pylon occurred in the neighborhood of 50-62.5% semispan position, just as with the fences. Also shown in Fig. 10 (bottom curve) is the additional improvement due to two vortex generators (not necessarily in the optimum positions), albeit at the cost of increased low-alpha drag.

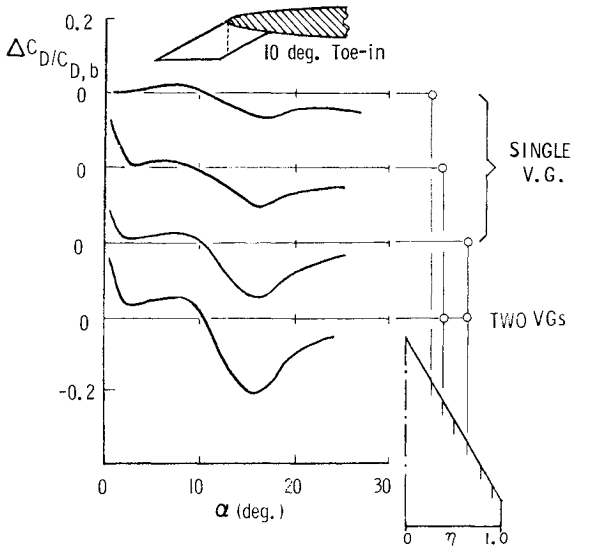

Fig. 10 Drag reduction with a single and two pylon vortex generators.

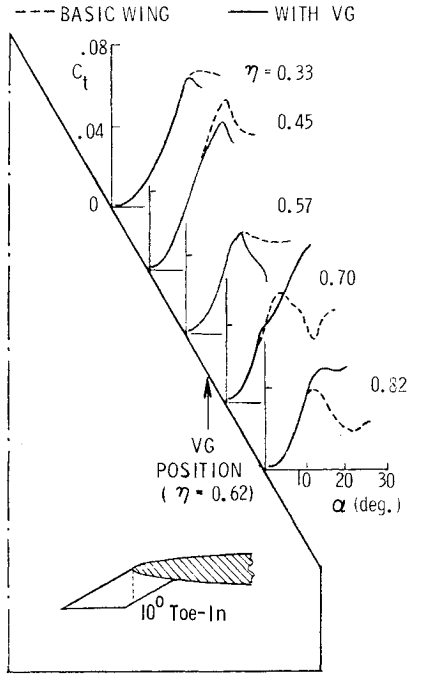

Fig. 11 Local leading-edge thrust characteristics with single pylon vortex generator.

Local leading-edge thrust characteristics with a single pylon vortex generator at 62.5% semispan are presented in Fig. 11. The stations closest to the pylon location clearly indicate the vortex-induced effects starting at $\alpha = 12$ deg approximately, when C_l begins to drop at the inboard station but continues its rise outboard up to the highest angle of attack of the test.

Vortex Plate

The drag-reduction performance of vortex plate device with varying spanwise coverage on the thin leading-edge model is shown in Fig. 12. Starting with a full-span device, increasing lengths of the plate from the apex were cut away. With only the outer half of the semispan covered, the peak drag

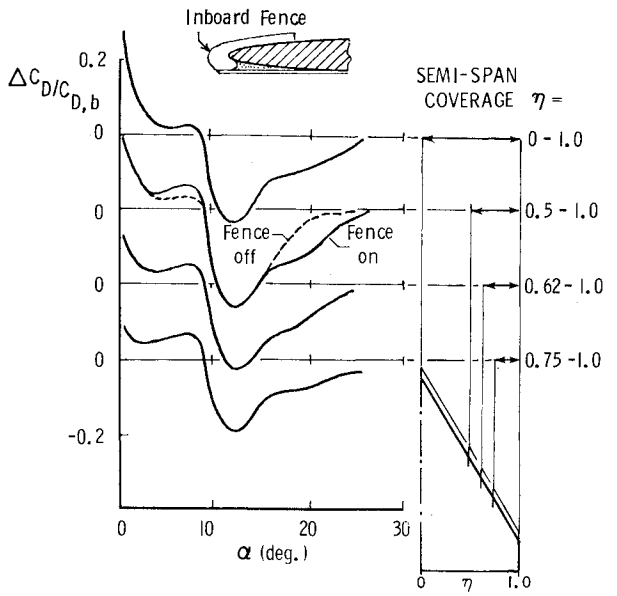

Fig. 12 Drag reduction with a vortex plate of varying spanwise coverage.

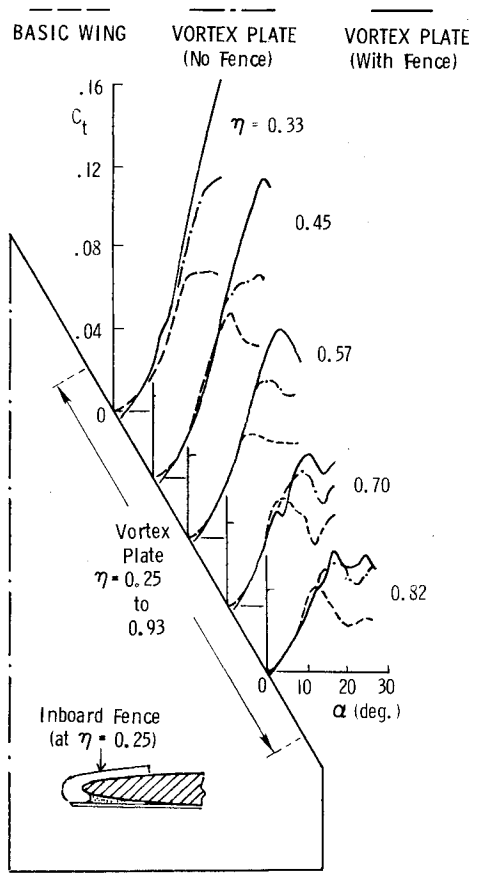

Fig. 13 Local leading-edge thrust characteristics with vortex plate.

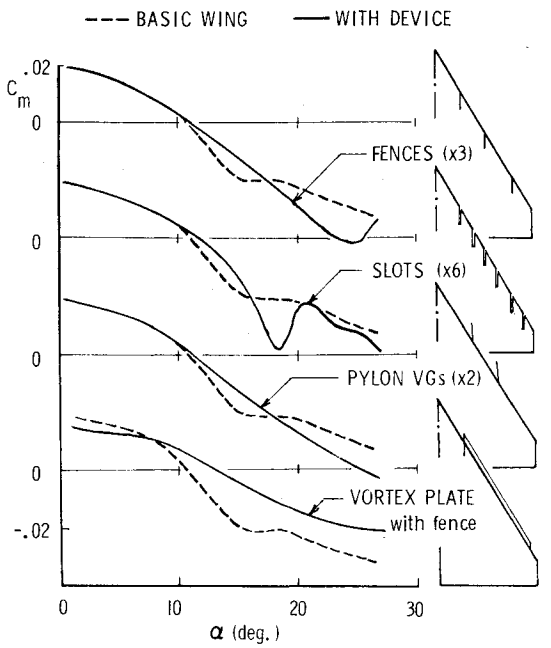

Fig. 14 Pitching-moment characteristics with various leading-edge devices.

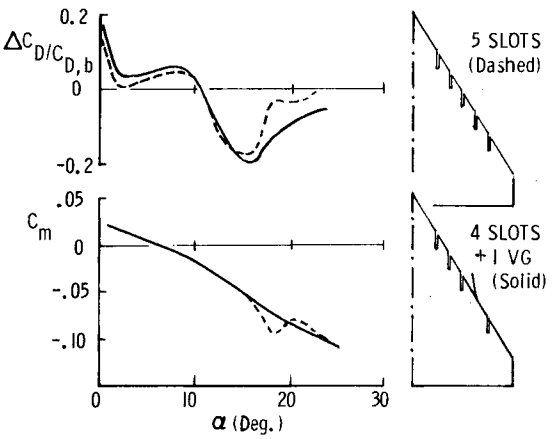

Fig. 15 Drag reduction and pitching-moment characteristics of slots/pylon vortex generator combination.

reduction (i.e., at $\alpha = 12$ deg) was actually improved over the full-span plate. The performance deficit (compared with full span at higher angles of attack) of the 50% vortex plate was compensated by adding a fence at the inboard end. The intent of the fence was to block the spanwise flow from the inboard half of the wing and allow a clean vortex to form on the plate. Further reductions in the vortex plate span coverage (with inboard fence attached) resulted in progressively reducing drag benefit. With only the outer one quarter of the semispan coverage, however, a 20% reduction in drag at $\alpha = 12$ deg was still obtained.

The local leading-edge thrust development with a vortex plate extending from 25 to 93% semispan on the thick leading edge are present in Fig. 13. The benefit due to the fence is particularly notable at the inboard stations, where C_l reached the highest levels recorded in the entire investigation. A weakening of the incremental thrust in the spanwise direction suggests an expanding vortex core, which gradually forces itself off the plate and moves over to the wing. In this case, additional fences spaced along the semispan may allow fresh vortices to be generated to improve the vortex plate effectiveness in the outboard regions.

Longitudinal Stability

As already noted in Fig. 3, the basic wing indicated a longitudinal instability as the leading-edge flow separation and attendant vortex lift moved forward of the c.g. It was anticipated that leading-edge devices that successfully delayed separation also would postpone the instability onset. The pitching-moment measurements obtained with particular device arrangements representing effective drag reducers are compared with the basic wing data in Fig. 14. Pylon vortex

generators and vortex plate are seen to eliminate the instability entirely in the angle-of-attack range of the test, while the three fence arrangement delays it substantially. The slots on the other hand aggravated the pitch up due to a sudden collapse of attached flow over most of the leading edge behind the c.g. It was found that this adverse characteristic could be alleviated considerably by replacing one of the slots with a vortex generator, which yielded a corresponding improvement in the drag-reduction performance at high angles of attack, Fig. 15. This is one example of the possibilities of device combinations for even better overall performance than obtainable with any single type.

Concluding Remarks

Four leading-edge flow manipulator concepts for high-alpha drag reduction have been explored in wind tunnel tests on a 60 deg cropped delta wing. The devices represented three basically different approaches: a) modifications of leading-edge upwash to obtain a camber effect (fences and pylon vortex generator); b) compartmenting the swept leading edge into "two-dimensional" segments (chordwise slots); and c) forced separation to produce a coiled vortex in front of the leading edge for generating thrust as an alternative to attached-flow suction. Selected experimental results have been presented to illustrate the unique aerodynamic mechanisms and drag-reduction potential of each class of device. Although this exploratory study emphasized concept evaluation rather than optimization, drag reductions as high as 25% at high angles of attack were demonstrated. The vortex plate showed considerable promise and potential for further development particularly as a retractable device to eliminate cruise-drag penalty. The devices (or their combinations) also successfully alleviated the longitudinal instability of the basic wing. Further investigations are needed to evaluate the effect of these devices on the lateral stability of delta wings at high angles of attack.

Acknowledgment

Research described herein was supported by NASA Langley Research Center.

References

[1] Robins, A. W. and Carlson, H. W., "High-Performance Wings With Significant Leading-Edge Thrust at Supersonic Speeds," *Journal of Aircraft*, Vol. 17, June 1980, pp. 419-422.

[2] Furlong, G. C. and McHugh, J. G., "A Summary and Analysis of the Low-Speed Longitudinal Characteristics of Swept Wings at High Reynolds Number," NACA TR 1339, 1957.

[3] Kuchemann, D., "Types of Flow on Swept Wings," *Journal of the Royal Aeronautical Society*, Vol. 57, Nov. 1953, pp. 683-699.

[4] Rao, D. M. and Johnson, T. D., Jr., "Subsonic Wind-Tunnel Investigation of Leading-Edge Devices on Delta Wings (Data Report)," NASA CR 159120, 1979.

[5] Lamar, J. E. and Gloss, B. B., "Subsonic Aerodynamic Characteristics of Interacting Lifting Surfaces with Separated Flow Around Sharp Edges Predicted by a Vortex-Lattice Method," NASA TN D-7921, 1975.